Marine Geology xxx (2009) xxx–xxx

Contents lists available at ScienceDirect

Marine Geology

journal homepage: www.elsevier.com/locate/margeo

The structures beneath submarine methane seeps: Seismic evidence from Opouawe Bank, Hikurangi Margin, New Zealand

G.L. Netzeband *[,1], A. Krabbenhoeft [2], M. Zillmer [3], C.J. Petersen [4], C. Papenberg [5], J. Bialas [6]

IFM-GEOMAR, Wischhofstraße 1-3, 24148 Kiel, Germany

ARTICLE INFO

Article history:
Received 15 July 2008
Received in revised form 5 July 2009
Accepted 9 July 2009
Available online xxxx

Communicated by G.J. de Lange

Keywords:
seeps
vents
seismics
methane
gas hydrate
mound
Hikurangi Margin
Opouawe Bank
Wairarapa area

ABSTRACT

The role of methane in the global bio-geo-system is one of the most important issues of present-day research. Cold seeps, where methane leaves the seafloor and enters the water column, provide valuable evidence of subsurface methane paths. Within the *New Vents* project we investigate cold seeps and seep structures at the Hikurangi Margin, east of New Zealand. In the area of Opouawe Bank, offshore the southern tip of the North Island, numerous extremely active seeps have been discovered. High-resolution seismic sections show a variety of seep structures. We see seismic chimneys either characterised by high-amplitude reflections or by acoustic turbidity and faults presumably acting as fluid pathways. The bathymetric expression of the seeps also varies: There are seeps exhibiting a flat seafloor as well as a seep located in a depression and small mounds.

The images of the 3.5 kHz Parasound system reveal the near-surface structure of the vent sites. While high-amplitude spots within the uppermost 50 m below the seafloor (bsf) are observed at the majority of the seep structures, indicating gas hydrate and/or authigenic carbonate formations with an accumulation of free gas underneath, a few seep structures are characterised by the complete absence of reflections, indicating a high gas content without the formation of a gas trap by hydrates or carbonates. The factors controlling seep formation have been analysed with respect to seep location, seep structure, water depth, seafloor morphology, faults and gas hydrate distribution. The results indicate that the prevailing structural control for seep formation at Opouawe Bank is the presence of numerous minor faults piercing the base of the gas hydrate stability zone.

1. Introduction

Focused fluid flow in marine sediments is a worldwide phenomenon. Although it has been the subject of numerous recent studies all over the world, it is not yet really understood (e.g. Eichhubl et al., 2000; Berndt, 2005; Dupré et al., 2007). In particular, the impact of methane release at the seafloor on the global carbon cycle is still under debate (Judd et al., 2002; Etiope and Klusman, 2002; Etiope et al., 2007). Seabed methane escape occurs at coasts (estuaries, bays, drowned valleys, deltas, etc.), continental shelves (faults, breached antiforms, salt diapirs), continental slopes and rises, deep oceans and convergent plate boundaries (Judd, 2003). Topographic expressions of fluid expulsion at the seafloor range from build-ups (mud volcanoes, carbonate mounds) to depressions (pockmarks) (Mazurenko and Soloviev, 2003; Berndt, 2005). In general, the distribution of fluid seeps is controlled by buried underlying features such as major faults, polygonal faults, salt diapirs, erosional surfaces and palaeo-channels (Gay et al., 2007). Fluid expulsion has been inferred as a factor in slope instability (Collot et al., 2001; Lewis et al., 1998; Cochonat et al., 2002). Furthermore, a link between methane seepage and gas hydrate reservoirs has been discussed by several authors (e.g. Mazurenko and Soloviev, 2003; Gay et al., 2007).

In this study, we focus on seep structures at the Hikurangi Margin, offshore New Zealand. Within the New Vents project, a number of active seeps have been discovered at Opouawe Bank (Greinert et al., this issue; Klaucke et al., this issue; Schwalenberg et al., this issue; Krabbenhoeft et al., this issue). The main objectives in investigating these seeps are the relation between seep locations and gas hydrate deposits, indicated by a bottom simulating reflection (BSR), and to understand their structural control on the observed seep structures, their seafloor topography, their location and the subsurface fluid pathways. In order to distinguish between the seeps as a seafloor

* Corresponding author. Tel.: +49 40 6375 2567.
E-mail addresses: gesa.netzeband@rwe.com (G.L. Netzeband), akrabbenhoeft@ifm-geomar.de (A. Krabbenhoeft), matthias.zillmer@eost.u-strasbg.fr (M. Zillmer), joerg.petersen@rwe.com (C.J. Petersen), cpapenberg@ifm-geomar.de (C. Papenberg), jbialas@ifm-geomar.de (J. Bialas)
[1] Now at: RWE Dea, Überseering 40, 22297 Hamburg, Germany.
[2] Tel.: +49 431 600 2325; fax: +49 431 600 2922.
[3] Now at: Institute de Physique du Globe de Strasbourg (IPGS), 5 Rue René Descartes, 67084 Strasbourg, France. Tel.: +33 90240088.
[4] Now at: RWE Dea, Überseering 40, 22297 Hamburg, Germany. Tel.: +49 40 6375 2580.
[5] Tel.: +49 431 600 2330; fax: +49 431 600 2922.
[6] Tel.: +49 431 600 2329; fax: +49 431 600 2922.

0025-3227/$ – see front matter © 2009 Elsevier B.V. All rights reserved.
doi:10.1016/j.margeo.2009.07.005

phenomenon and their subsurface signature as observed in the seismic sections, the subsurface phenomenon will be called 'seep structure'. It will be indicated where a seeps structure can be unequivocally linked to a seep observed at the seafloor.

2. Geological setting

The authors refer to Barnes et al. (this issue) for a detailed description of the geological background and a tectonic map as well as Greinert et al. (this issue) for an overview of the multidisciplinary cruises undertaken in 2006 and 2007 to Opouawe Bank. The following comprises only a brief introduction to the area. The research area is located at the Hikurangi Margin, on the continental slope (Fig. 1). The Hikurangi Margin, off North Island and the southern tip of South Island, New Zealand, is the southernmost expression of the Tonga–Kermadec subduction zone of the SW Pacific. In this part, the subduction started at about 21 Ma (Field et al., 1997). Because of the movement of the rotation pole of the Pacific Plate the subduction is highly oblique (e.g. Robinson, 1986; Walcott, 1987; Collot et al., 1996). Plate convergence decreases southwards along the margin until at ~42°S strike-slip motion dominates and subduction occurs no more (e.g. Reading et al., 2001).

Barnes and Mercier de Lépinay (1997) identified and dated 8 sedimentary horizons in deep water in the area around the south-eastern tip of the North Island. They derived an accumulation rate of compacted sediment of 0.65 mm/a for the Quaternary trench fill in front of the wedge. A sedimentation rate of 0.42 mm/a is assumed for the time between 0.8 Ma and 2 Ma and a rate of 0.3 mm/a between 2 Ma and 5 Ma.

Gas hydrate occurrences at the Hikurangi Margin have been investigated by several authors (e.g. Katz, 1981, 1982; Pecher et al., 2004, Pecher et al., 2005). An extensive BSR has been observed along the entire margin (Townend 1997). Lewis and Marshall (1996) were the first to collate evidence of seep faunas, bubble plumes, and seabed carbonate chimneys and mats from around New Zealand and to relate them to tectonic setting. Pecher et al. (2004) have investigated the coexistence of gas hydrates and gas conduits for seeps within the gas hydrate stability zone (GHSZ) at the Hikurangi Margin and postulated ample methane supply at these venting systems. Faure et al. (2006) analysed seeps and BSR occurrence in Rock Garden offshore Hawke's Bay and found that gas hydrates are probably a controlling factor for seepage and seafloor stability along the Hikurangi Margin. Kvenvolden and Pettinga (1989) analysed two onshore seeps near Hawke's Bay. They demonstrated that gas compositions of both seeps are different from geothermal gases, proving that they are not influenced by volcanic-related geothermal processes and thus do not originate from great depths. By calculating thermal gradients from the BSR depths at Rock Garden using different gas compositions, Faure et al.

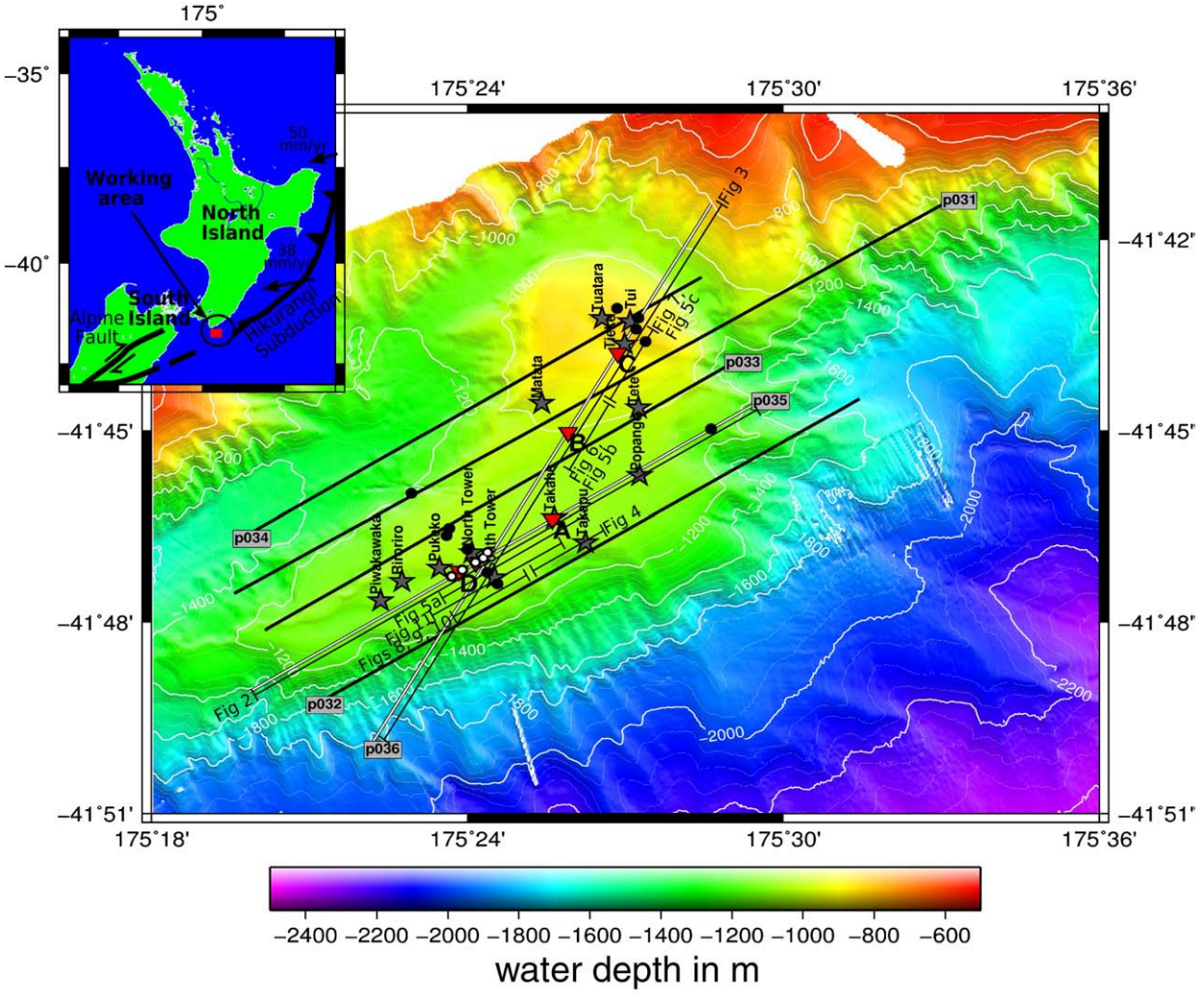

Fig. 1. Map of study area. The location is shown in the inset. Annotated arrows indicate the direction and amount of plate motion, half arrows indicate transform/strike-slip faults (after Barnes and Mercier de Lépinay, 1997). Black lines indicate multichannel seismic profiles. Black circles mark OBS locations, the five OBS stations used for migration (compare Fig. 10) are indicated by white circles. Profile numbers and OBS numbers are annotated. Bathymetry was acquired from Simrad system during cruise SO190. Previously known seeps are marked in the map by grey stars. Seep Structures discussed in this paper are indicated by white triangles.

Please cite this article as: Netzeband, G.L., et al., The structures beneath submarine methane seeps: Seismic evidence from Opouawe Bank, Hikurangi Margin, New Zealand, Mar. Geol. (2009), doi:10.1016/j.margeo.2009.07.005

(2006) concluded that the gas composition of the offshore seeps is most probably not pure methane. A composition similar to the average of 21 onshore seeps (96% CH_4, 2.6% CO_2, 1.1% ethane, 0.3% propane, 3.5% NaCl) analysed by Giggenbach et al. (1993) is more likely. The same composition without propane is also possible according to Faure et al. (2006). Pecher et al. (2005) found evidence at Rock Garden and Ritchie Banks for the composition without the propane fraction. However, no detailed studies have been made of the gas composition of gas hydrates at Opouawe Bank, although hydrates were recovered in 2007 (Schwalenberg et al., this issue).

Heat flow estimates at the central Hikurangi accretionary prism reveal average values around 45 mW/m^2 (Townend, 1997, Henrys et al., 2003). Local anomalies are found on the crest of anticlines (reduced heat flow values) and on steep flanks (high values). The surface heat flow reveals anomalies of up to 10 mW/m^2 where the bathymetry exhibits steep slopes (Henrys et al., 2003).

3. Materials and methods

The data of this study were collected during cruise SO191-1 with the German research vessel *RV SONNE* in 2007. Six multichannel seismic (MCS) reflection lines between 14 and 20 km length were recorded in the research area (Fig. 1). The profiles were recorded with a 4-channel streamer of 36 m active length, a group distance of 12 m and a maximum source–receiver offset of 83 m. The sampling rate was chosen as 1 ms. The source was a single GI-Gun with a volume of 250/105 in^3, which was operated in harmonic mode. The shot interval was 14 s, which corresponds to an average spacing of about 22 m for a ship speed of 3 kn.

The recordings were sorted for common mid-points (CMPs) with a CMP spacing of 20 m, then stacked and band pass filtered with passing frequencies between 16 and 120 Hz. Because of the short offset, a velocity analysis could not be performed. A time migration was applied with a constant migration velocity of 1500 m/s. During data acquisition, the pre-amplifier of the data recorder was temporarily not working properly, which resulted in overamplification of the seafloor reflection and of some other samples, especially on line P036. These over-amplified blocks were removed where possible, leaving 'smileys' in the migrated section (e.g. 7.3 km, 8.5 km, 11 km, 11.3 km, 13.2 km).

Parasound data were acquired along all profiles. The onboard Parasound system worked with a frequency of 3.5 kHz, hence the shallow sediment sequences are better resolved than in the MCS sections due to the higher source frequency. However, the penetration depth is limited to a few tens of meters. Furthermore, a deep-towed Edgetech DW-216 chirp subbottom profiler (SBP) was operated in a frequency range of 2–8 kHz providing penetration depths of up to 50 m.

In addition to the MCS lines, 16 ocean bottom seismometers (OBS) were deployed in the working area (Fig. 1). The OBS data were acquired simultaneously with the MCS profiles thus having the same source parameters. All of the ocean bottom instruments worked flawlessly and recorded data. The sampling rate of the OBSs was 1 ms.

The OBS stations 22, 23, 26, 27 and 28 were positioned along MCS line P035 with a spacing of 200–430 m. The hydrophone components of these stations were used to develop a 2D velocity-depth model. The modeling was performed with the software package *rayinvr* of Zelt

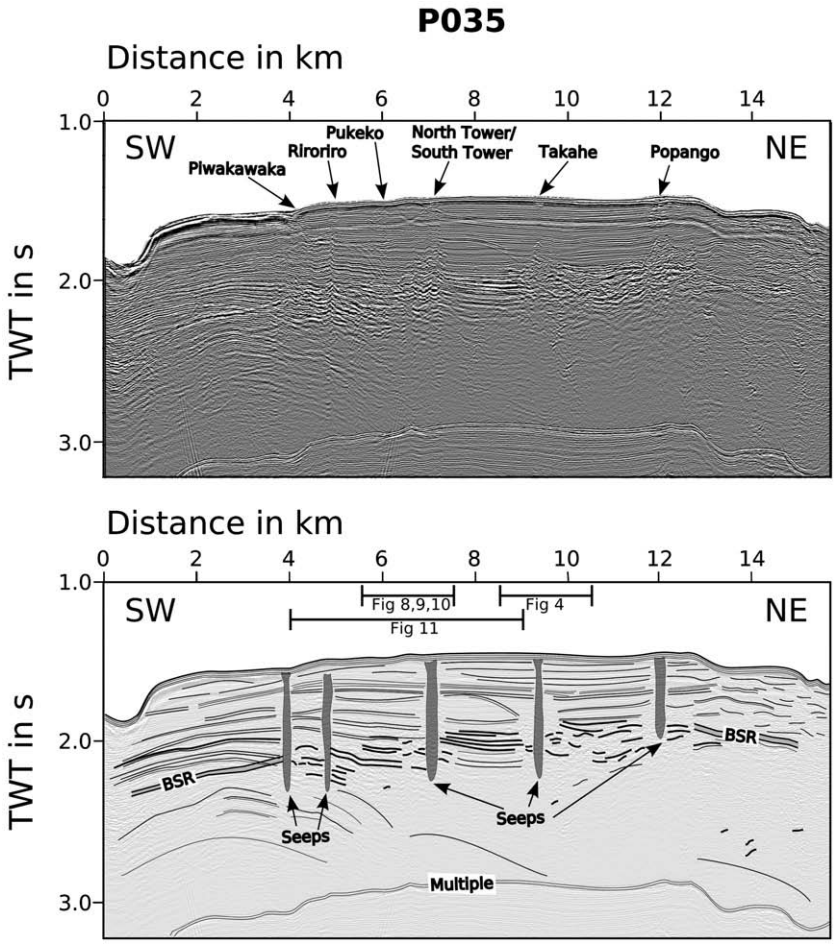

Fig. 2. Line P035 MCS profile; original above, interpretive line drawing below. The grey shaded columns indicate evidence of subsurface seep plumbing. The bottom simulating reflection (BSR), where observed, is shown by a filled double line.

Please cite this article as: Netzeband, G.L., et al., The structures beneath submarine methane seeps: Seismic evidence from Opouawe Bank, Hikurangi Margin, New Zealand, Mar. Geol. (2009), doi:10.1016/j.margeo.2009.07.005

and Smith (1992). A forward modeling technique was applied first. Its result served as the starting model for the inversion algorithm of *rayinvr*. For comparison, the MCS section was depth converted with a 1D velocity-depth function derived from the final *rayinvr* model near OBS site 23. The result was then plotted together with the velocity model.

The same wide angle data were used for Kirchhoff depth migration (Zillmer et al., 2005). The data of each station were migrated separately and subsequently concatenated into one image. The velocity model, which was used for the migration, consisted of 1D-sections taken from the inversion model at OBS site 23.

4. Observations and results

The seismic profiles P035 and P036 and a number of sections showing seep structures in detail are described in the following.

4.1. Seismic profiles P035 and P036

The seismic profiles P035 and P036 (Figs. 2 and 3) show a BSR at about 0.6 s below the seafloor (bsf), which is interrupted at a number of seep structures. Between these seep structures, the BSR level is characterised by several high-amplitude reflections, which are interpreted to coincide with the base of the gas hydrate stability zone (BGHSZ). On P035, the BSR is visible in the SW, on the first 4 km and also towards the NE between 13 km and 15 km. As expected, it runs parallel to the seafloor, except for the first km of the seismic line, where the seafloor abruptly changes its gradient, while the BSR keeps a constant dip angle, which indicates recent slumping. Below the BSR, only a few weak reflections are observed at the southwestern end of the line. Above the BSR, the reflections are subparallel to the seafloor. At some locations, the reflections change their dip angle with depth, e.g. from southwest of the seep structure at 4 km or near 8 km. At the northeastern end of line P035, the reflection pattern becomes hummocky. Significant faults are not observed, but a number of small fractures can be found throughout the line (Fig. 2). Multiple small fractures occur at seep structures, where they are generally accompanied by upward bending of adjacent reflections.

On line P036 (Fig. 3), the BSR is more pronounced than on P035, especially towards the SW, but also occurs intermittently between the seep structures, where it may occur as several high-amplitude reflections. Below the BSR, very few reflections are visible in the SW, which is in striking contrast to the NE end of line P036, where reflections up to 1.5 s bsf are well resolved. The stratigraphic pattern in the central part of the line is subparallel to the seafloor, as in P035. The dip angle varies along the line and also with depth. Towards the NE, the stratigraphy becomes more regular, while to the SW, hummocky clinoforms dominate. Here, the seafloor is irregular and is locally steeper than the BSR. Several seep structures are observed, with varied appearance. In the following, seep structures with different characteristics are described in detail.

4.2. Seep structures

At Seep Structure A (Fig. 4), which feeds seep Takahe, a seismic chimney of approx. 100 m width is observed beneath a flat seafloor at

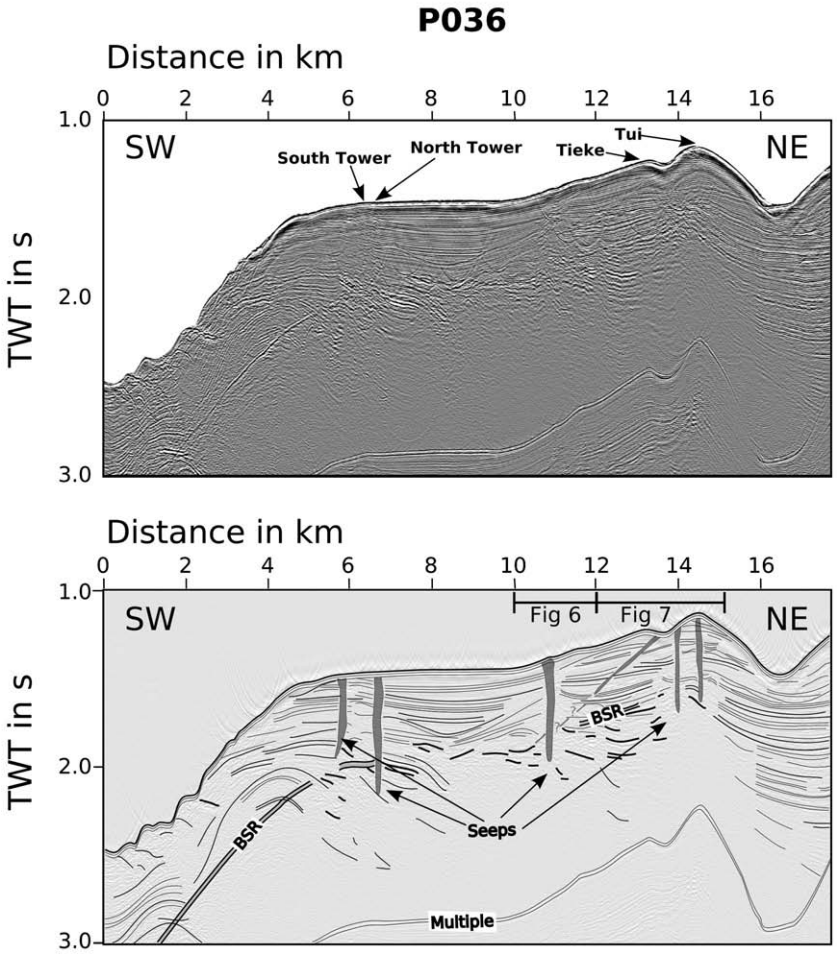

Fig. 3. Line P036 MCS profile; original above, interpretive line drawing below. The grey shaded columns indicate evidence of subsurface seep plumbing. The bottom simulating reflection (BSR), where observed, is shown by a filled double line.

Please cite this article as: Netzeband, G.L., et al., The structures beneath submarine methane seeps: Seismic evidence from Opouawe Bank, Hikurangi Margin, New Zealand, Mar. Geol. (2009), doi:10.1016/j.margeo.2009.07.005

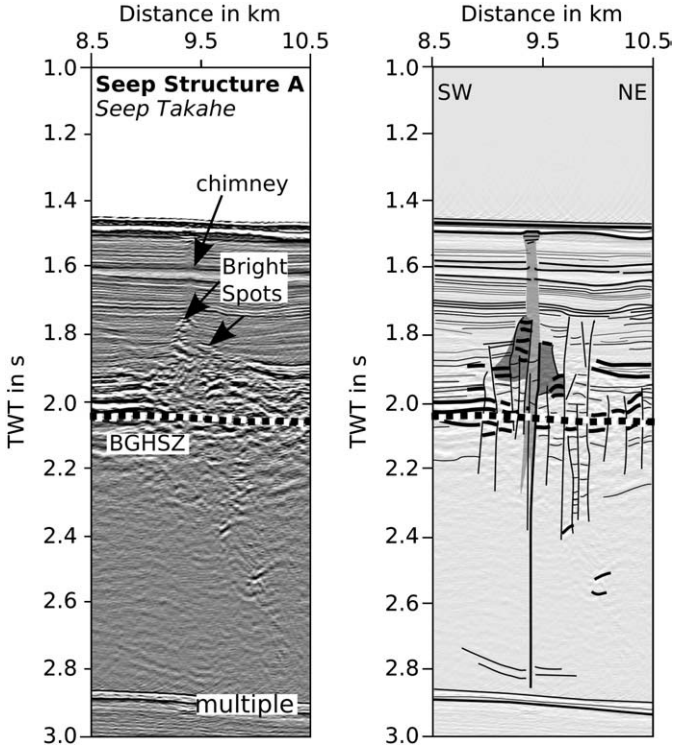

Fig. 4. MCS Seismic image and interpretive line drawing of Seep Structure A on P035. The seismic chimney with its acoustic wipe-out is marked by the area shaded in light grey. The dark grey denotes the region of enhanced reflections above the base of gas hydrate stability zone (BGHSZ). The BHGSZ itself is marked by the black-and-white line. Faults and fractures are indicated.

about 9.3 km. The reflections from beneath the seafloor down to the BSR level are suppressed. In general, the reflections are quite even, almost horizontal, and more or less follow the seafloor. However, in the vicinity of the chimney, the reflections are bent upwards. At the top of the chimney, right beneath the seafloor, a single high-amplitude reflection appears. The BSR level is characterised by several patchy high-amplitude reflections in a corridor between 1.9 and 2.1 s, except for the northeastern flank of the chimney, where these reflective patches occur as shallow as 1.7 s. There is evidence of a fault at this seep structure, which can be traced down to at least 2.8 s, but shows no expression at the seafloor. The Parasound image (Fig. 5a) shows a very confined increase in reflection amplitude in the first 10 m bsf, followed by a spot of reduced amplitude in the next 10 m. In the entire zone of Seep Structure A (9.2–9.5 km), the reflection amplitude below 20 m bsf is strongly reduced.

At Seep Structure B a short seismic chimney of approx. 200 m width is observed (Fig. 6), beginning at about 0.1 s bsf and terminating in a small mound rising about 5 m above the seafloor. The chimney is characterised by the absence of reflections. A zone of strong reflections surrounds this chimney. A fault can be traced from about 2.0 s bsf up to the seafloor, piercing the mound at its southwestern flank. Also a few small fractures occur. The reflections at the BSR level (1.9–2.0 s) look patchier and more disrupted than at Seep Structure A (Fig. 4). Southwest of the seep structure, the stratigraphy is characterised by weak hummocky reflections, while to the northeast, the reflections below 1.5 s appear quite irregular. The Parasound image (Fig. 5b) shows only slightly reduced reflectivity in the upper 10 m bsf, but reflections below 10 m bsf are suppressed at the seep site.

At Seep Structure C, there seem to be three seeps at the seafloor (Fig. 7). One located in the center of to a depression 25 m deep and 600 m wide, one on the flank and one on top of the bathymetric high. The latter two terminate in mounds of roughly 5 m in height. Only two seeps are observed on the seafloor, Tieke and Tui (Figs. 1 and 3). Beneath the dome, two vertical seismic chimneys are indicated by reduced reflection amplitudes, both accompanied by faults, which can be traced below the BGHSZ. Compared to other seep structures (Figs. 4 and 8), the reflections at the BGHSZ (approx. 1.6–1.7 s TWT) appear relatively weak, not stronger than the reflections above. Thus a BSR is not identifiable. The stratigraphy on the upper 0.3 s bsf seems almost undisturbed while the deeper reflections are contorted near the seep structures. The third seep seems to be supplied by a chimney, dipping at only ~6° to the SW (assuming a velocity of 1500 m/s). This seems to be associated with a normal fault. In the Parasound section, bright reflection patches appear at the seafloor at all three identified seep locations, accompanied by reduced reflection amplitudes underneath (Fig. 5c).

At Seep Structure D (Fig. 8) a small area of reduced amplitude is observed beneath a small mound of about 8 m height. A typical seismic chimney reaching down to the BGHSZ is not visible. At 7 km, the seismic section reveals a seep structure. Reflections are shifted upwards and a bright reflection appears right beneath the flat seafloor. The patchy high-amplitude reflections at the BGHSZ appear particularly disrupted beneath the seep location. Unlike the seismic image, there is almost no indication of a seep structure next to the mound in the Parasound image (Fig. 5a). Only the reflection at about 20 m bsf is slightly enhanced. But beneath the mound, all reflections are absent and only a single strong reflection occurs at 30 m bsf. The SBP image (Fig. 9) gives a more detailed view of both structures. Around 6.5 km, beneath the mound, not only blanking is observed, but a high-amplitude reflection at approx. 25 m bsf. This high-amplitude reflection exhibits two small summits, one at 6.4 km, the other at 6.7 km, both elevated by approx. 4 m. To the NE, two stratigraphic reflections are observed at 15 m bsf. Beneath the seep structure at 7 km, these reflections are partly obscured by high-amplitude reflections, rising from the reflection up to 10 m bsf.

The Kirchhoff depth migration of 5 OBS sections at seep structure D on P035, around profile km 7 (Fig. 10) confirms the interpretation from the MCS section. Reflections are blurred or contorted near the seep structure around profile km 7. A very pronounced fault becomes evident between 7.3 and 7.4 km. Steep low-amplitude reflections can be seen on both flanks of the seep structure. Below the mound at 6.5 km, nothing conspicuous is observed in the upper 400 m bsf, only a vertical jump in the reflections below occurs. Further information on the seep structure is provided by the velocity field (Fig. 11). Beneath the mound, the velocity is reduced from 1.6 to 1.7 km/s to only 1.5 km/s. There is no significant velocity anomaly at the seep structure at 7 km.

4.3. BSR and heat flow

A BSR appears on all profiles except P034. Where it is not continuously observed, it has been interpolated on the assumption that the high-amplitude reflections at the BSR level mark the BGHSZ. This interpolation provided a continuous basis to calculate heat flow (Fig. 12). Heat flow values have been calculated using the software CSMHYD (Sloan, 1998) to calculate thermal gradients. The thermal gradients were then multiplied with a thermal conductivity. The depth-dependent thermal conductivity was estimated on the basis of the calculations of Townend (1997) using the same parameters (2.8 W/m K as matrix conductivity and 0.6 W/m K as the conductivity of water) and then taking the average of the resulting conductivities, 1.2 W/m K. We assumed the gas composition determined by Giggenbach et al. (1993) from the analysis of 21 onshore seeps and favoured by Faure et al. (2006) for the Rock Garden area (96% CH_4, 2.6% CO_2, 1.1% ethane, 0.3% propane, 3.5% NaCl corresponding to Structure-II-hydrate). However, it should be noted that the general trend of heat flow values does not show much difference if Structure-I-hydrate or pure methane hydrate is assumed. The calculated values range between 40 and 55 mW/m^2, increasing with decreasing water

Please cite this article as: Netzeband, G.L., et al., The structures beneath submarine methane seeps: Seismic evidence from Opouawe Bank, Hikurangi Margin, New Zealand, Mar. Geol. (2009), doi:10.1016/j.margeo.2009.07.005

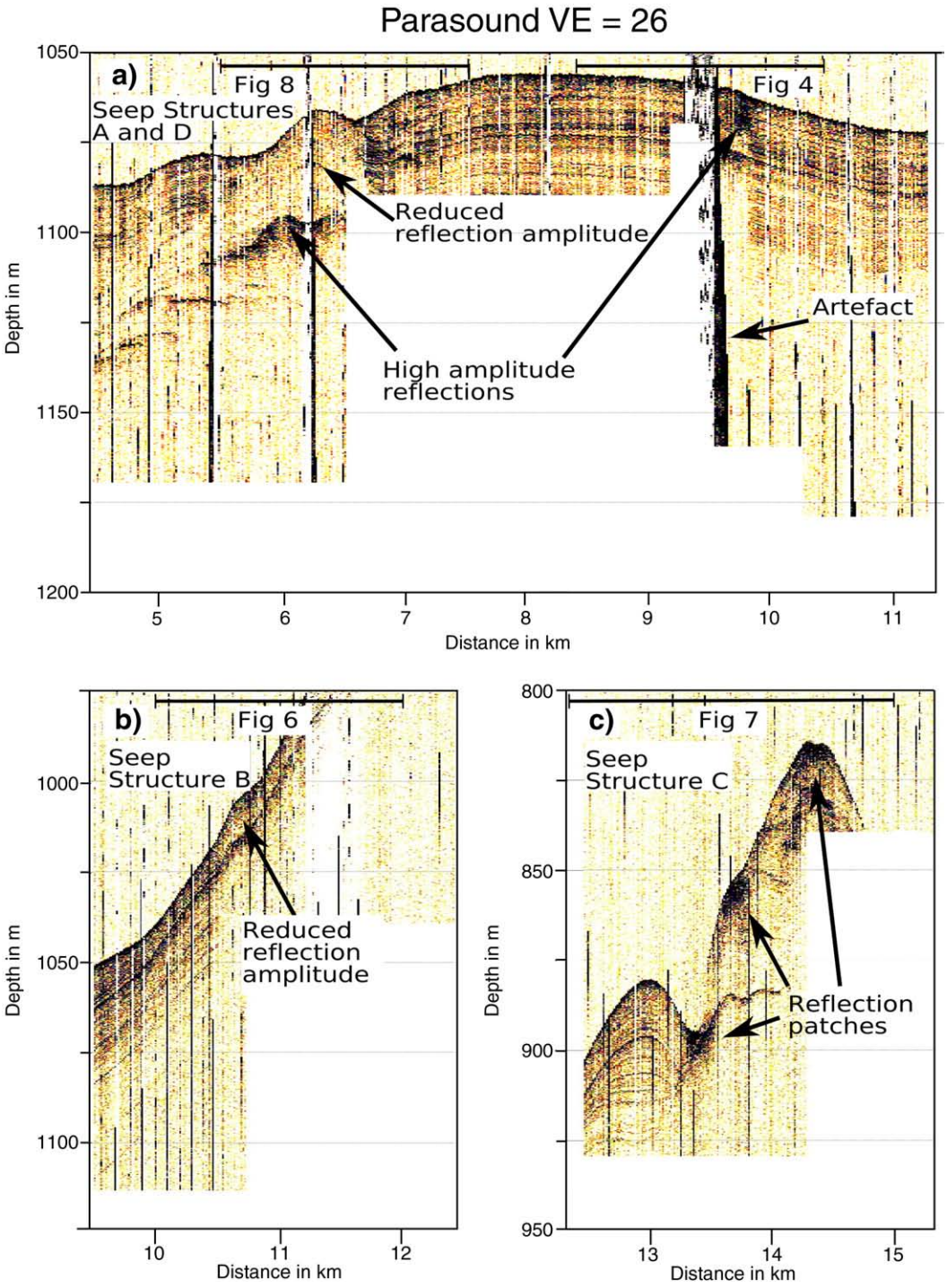

Fig. 5. Parasound images of seep structures. Note the vertical exaggeration (VE = 24). a) Seep Structure s A and D on line P035. The image of Seep Structure A is partly disturbed by an acquisition artefact. Note the difference of the reflection characteristics underneath both seep structures. b) Seep Structure B on line P036. Note how the reflection pattern changes near the seep. c) Seep Structure C on line P036. Sediment layers, as observed near 13 km, are not resolved below the three prominent reflection patches.

depth, except for the SW parts of e.g. P036, where we see evidence of slumping.

5. Discussion

In general, seep structures as observed in the study area can be pathways for overpressured pore fluids generated by sediment compaction or pathways for free gas, i.e. methane and higher hydrocarbons. We have measured significant methane concentration at some seeps (Faure et al., this issue; Krabbenhoeft et al., this issue; Sommer et al., this issue) and recorded flares in the water column above some of the 9 seep at Opouawe Bank studied in detail. The presence of a BSR indicates that there is gas hydrate and thus a sufficient supply of methane to form the hydrate. Below the BSR, and below the reflection band marking the BGHSZ near the seep structures, we observe a noticeable signal attenuation. E.g. in the NE of P036 (Fig. 3), where neither seeps nor BSR occur, the seismic section shows a sediment package of more than 1.5 s TWT, while in the central parts of this line, and also in the central

Please cite this article as: Netzeband, G.L., et al., The structures beneath submarine methane seeps: Seismic evidence from Opouawe Bank, Hikurangi Margin, New Zealand, Mar. Geol. (2009), doi:10.1016/j.margeo.2009.07.005

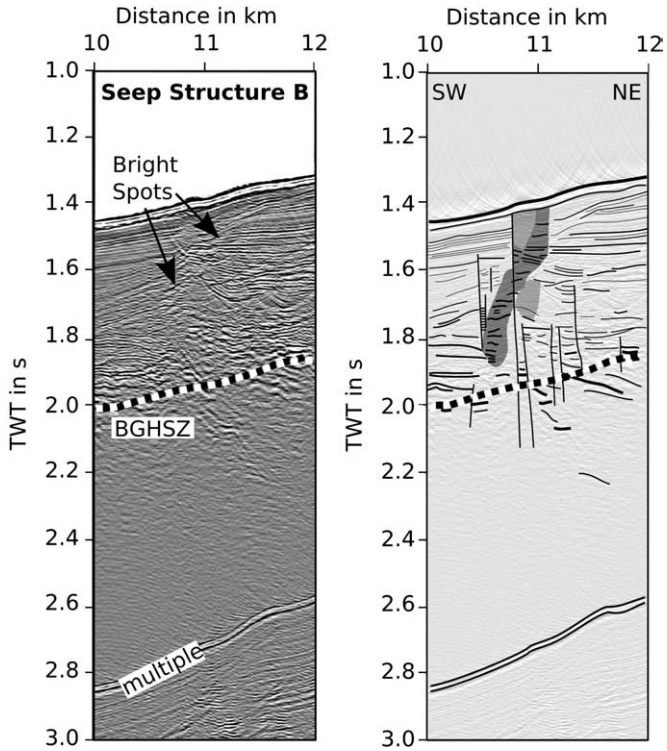

Fig. 6. MCS Seismic image and interpretive line drawing of Seep Structure B on P036. The regions of acoustic blanking are marked by the areas shaded in light grey. The dark grey denotes the region of enhanced reflections above the BGHSZ. The BHGSZ is marked by the black-and-white line. Faults and fractures are indicated.

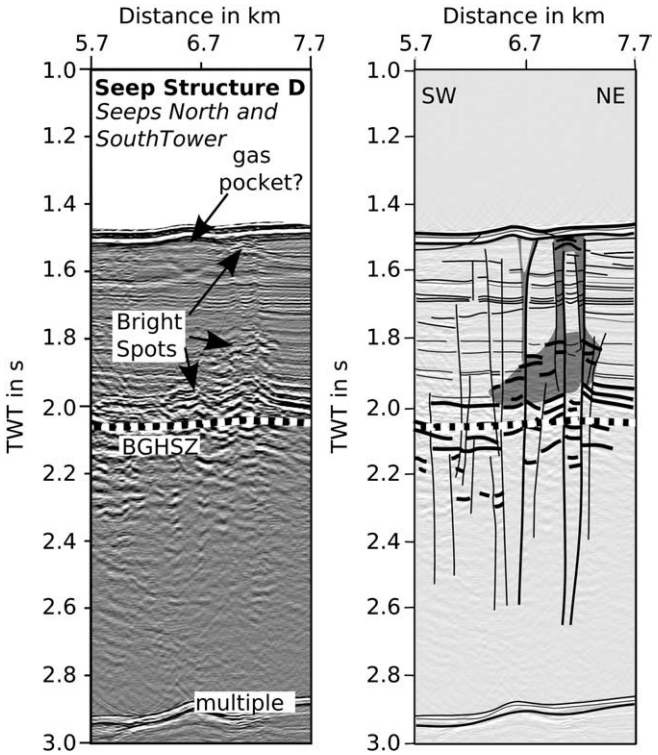

Fig. 8. MCS Seismic image and interpretive line drawing of Seep Structure D on P035. Note the absence of a seismic chimney with acoustic wipe-out. The dark grey denotes the chimney-like region of enhanced reflections and upward bulging above the BGHSZ. The BHGSZ is marked by the black-and-white line. Faults and fractures are indicated. The interpretation of a gas pocket at about 6.5 km is supported by Figs. 5a and 9.

part of P035 (Fig. 2), the reflectivity is strongly reduced below the BGHSZ. This suggests a large gas accumulation below the BGHSZ.

We observe shallow, patchy high-amplitude reflections at a number of seep structure s (e.g. Seep Structures A, C, D), which could be associated with carbonate crusts linked with methane flow. They could also originate from gas hydrate lenses formed in situ, from the interface between gas hydrate and free gas beneath. We therefore suppose that

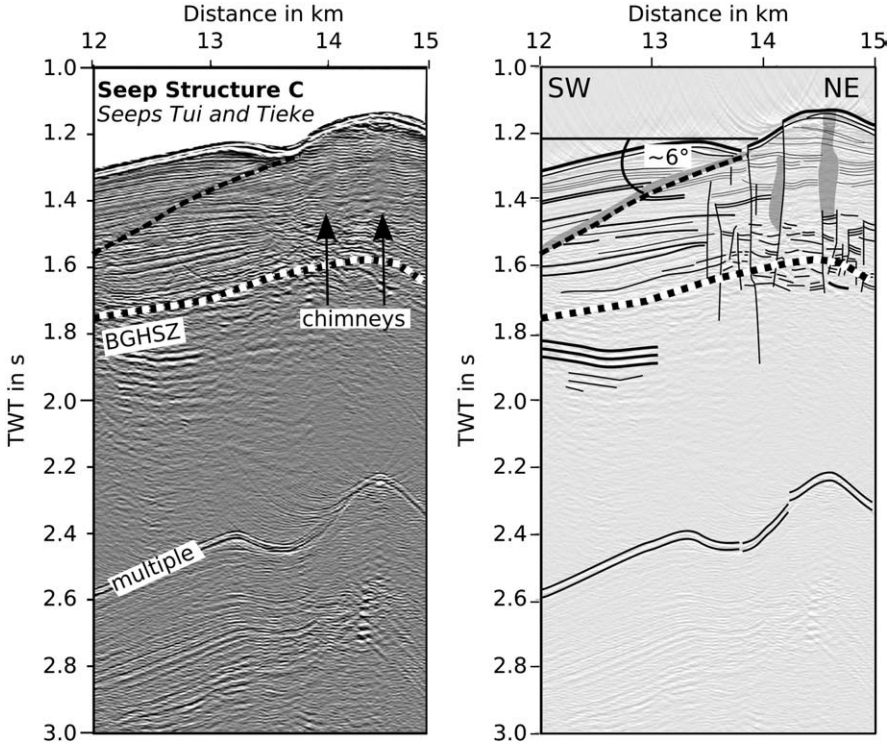

Fig. 7. MCS Seismic image and interpretive line drawing of Seep Structure C on P036. The regions of acoustic blanking are marked by the areas shaded in light grey. Faults and fractures are indicated. Note the slant chimney/fault plane, which is marked by a dashed black line. The BHGSZ is marked by the black-and-white line. Faults and fractures are indicated.

Please cite this article as: Netzeband, G.L., et al., The structures beneath submarine methane seeps: Seismic evidence from Opouawe Bank, Hikurangi Margin, New Zealand, Mar. Geol. (2009), doi:10.1016/j.margeo.2009.07.005

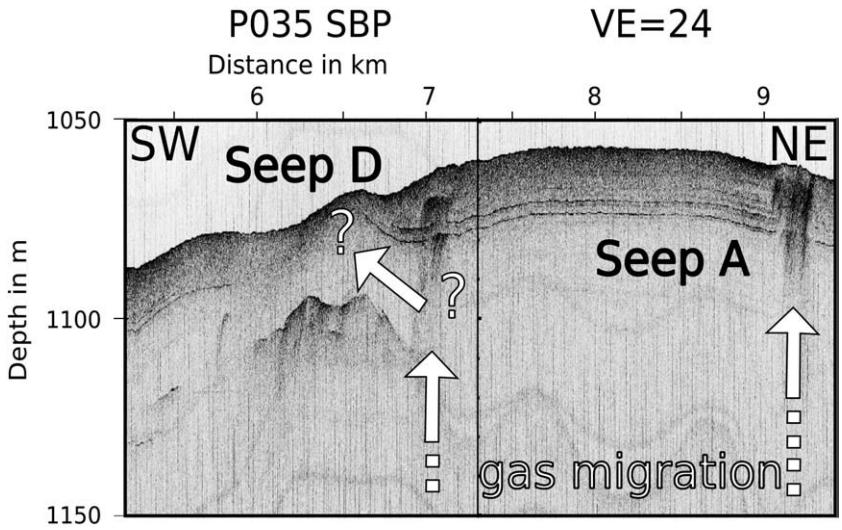

Fig. 9. Subbottom Profiler image of Seep D on P035. Note the same vertical resolution (24) as in the Parasound sections (Fig. 5). Besides the vertical gas migration (white arrows), there are also indications of near-horizontal migration. The reduced reflection amplitude beneath the seafloor at about 6.5 km is interpreted as a gas pocket, while the reflection patch in 1100 m depth is interpreted as buried carbonate. This would be impermeable to uprising fluids, which suggests that the gas transport to the shallow gas must come from the side.

all the observed seep structures represent conduits for methane gas, although additional pore water may also be involved.

5.1. Occurrence of seep structures in the subsurface

28 seep structures in the subsurface have been observed on all six profiles, which cover about 150 km^2. This corresponds to roughly 18 seeps/100 km^2. Since this is only a 2D survey, this is a minimum value. The seepage activity of an area cannot be deduced from the seep density alone, because the size of the seeps can vary by orders of magnitude (Hovland et al., 2002) as well as the venting intensity (e.g. Eichhubl et al., 2000). However, the concentration of seep structures places Opouawe Bank among the most active methane venting fields in the world, comparable with e.g. the Lower Congo Basin, where Gay et al. (2007) found 20 pockmarks per 100 km^2 in a 3D seismic survey. Almost half of the seep structures detected geophysically at Opouawe Bank have been identified by multibeam, multibeam backscatter and sidescan (Greinert et al., this issue; Klaucke et al., this issue). Five sites have been identified as actively releasing gas (Greinert et al., this issue).Several more showed signs of recent seepage activity 10 m below the mudline, which is below the seismic resolution. The difference in resolution is also the explanation for the different number of seep structures found e.g. in the seismic sections (this paper) and in the sidescan data (Klaucke et al., this issue) of Opouawe Bank.

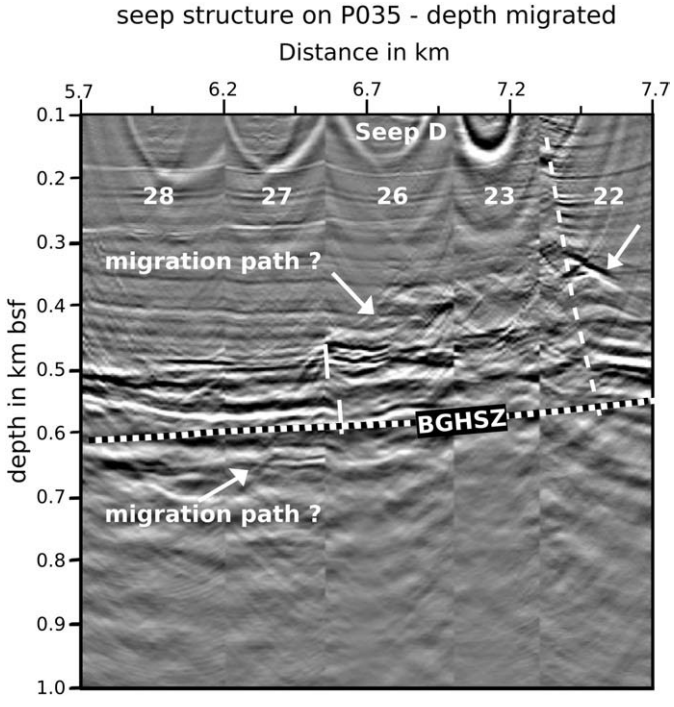

Fig. 10. Depth migrated seismic image of Seep Structure D based on five OBS sections. These sections were migrated separately and subsequently combined into one image, the individual sections are marked by white numbers. A prominent fault appears in this image at km 7.3–7.5, marked by the dashed white line. Smaller faults or fractures revealed by a vertical offset, indicated by the solid white lines. The arrows mark reflections, interpreted as a possible gas migration path, sloping up towards the seep structure and crossing the BGHSZ, which is marked by the black-and-white lines.

The great variety of seep structures and their seafloor morphology at Opouawe Bank requires an analysis of the possible mechanisms controlling the structure and appearance of the seeps. Conceivable controlling factors are water depth, fault and fold structures, gas hydrate and free gas reservoirs and dip of stratigraphic layers.

Elsewhere, seeps occur in a great range of water depths (Rollet et al., 2006), from a few tens of meters (e.g. Schroot et al., 2005) to over 2000 m (e.g. Greinert et al., 2006a,b). In the Lower Congo Basin, most seeps occur in water depths greater than 550 m, which corresponds to the outcropping of the BGHSZ at the seafloor (Gay et al., 2007). This indicates a link between gas hydrate occurrence and seepage. Since the entire research area of our study lies well within a water depth in which gas hydrates are potentially stable, a relation between seep distribution and water depth could not be established. Nevertheless, there seems to be a relation between BSR occurrence and seep sites. The data of this study show a disrupted BSR at seep locations, while Hustoft et al. (2007) show gas chimneys with an intact BSR underneath, as well as gas chimneys with an apparent disruption of the BSR. Gay et al. (2007) present seismic sections where the BSR is deflected upwards beneath a seep by about 15–20 m. The fact that the BSR is disrupted at all seep structures in our seismic sections, may be attributed to the limited resolution of the data. Hustoft et al. (2007) and Gay et al. (2007) showed 3D-data sets with higher lateral resolution. But even where the BSR is very clear, e.g. in the SW of line P036 (Fig. 3), it terminates right at a seep structure, then continues and terminates at the next seep structure. This suggests a disturbance at the BGHSZ rather than a mere imaging effect. Thus, the existence of a seep structure appears to be coupled to

Please cite this article as: Netzeband, G.L., et al., The structures beneath submarine methane seeps: Seismic evidence from Opouawe Bank, Hikurangi Margin, New Zealand, Mar. Geol. (2009), doi:10.1016/j.margeo.2009.07.005

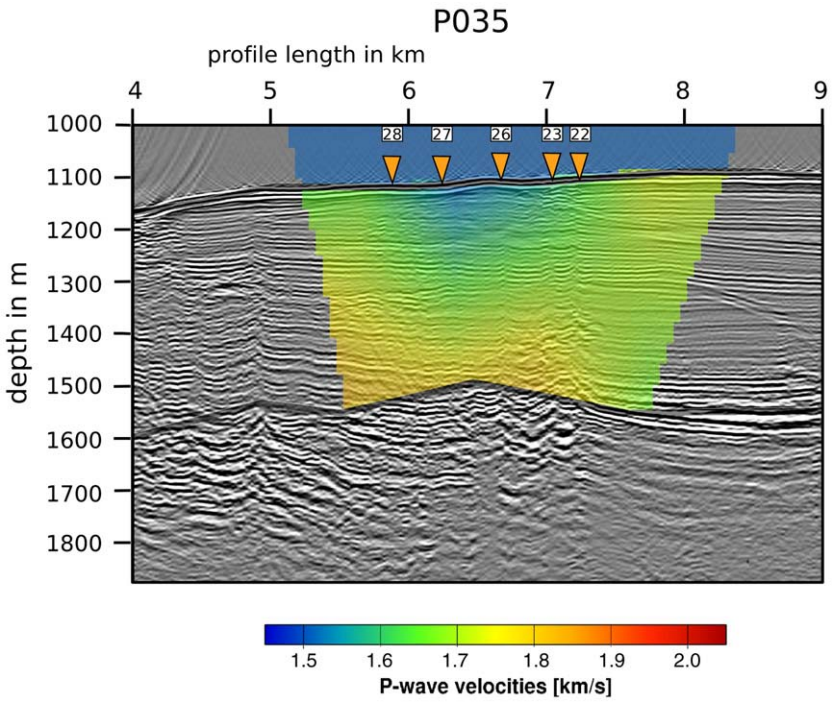

Fig. 11. Depth converted seismic image of Seep Structure D, overlain by the 2D-velocity field obtained from the same five OBS Sections in this figure. The OBS numbers are annotated. The velocity field, note the scale below, was derived by the raytracing method of Zelt and Smith (1992). A single layer with a velocity gradient was assumed between the seafloor and the BGHSZ. Note the low velocities beneath the seafloor between OBS 26 and OBS 27.

the absence of the BSR. This could imply that the rising fluids inhibit the formation of gas hydrates by perturbing the temperature field, as suggested by Pecher et al. (2005).

Several workers (Eichhubl et al., 2000; Gay et al., 2006; Rollet et al., 2006) have suggested a relation between fluid venting and buried channels or between slumping and fluid venting (Eichhubl et al., 2000; Cochonat et al., 2002). We observe a buried paleo-canyon on lines P033, P034, P035, P036, but no evidence of seepage on its flanks on either of these lines (Figs 2 and 3). There are also several indications of slumps in the study area with no evidence of seep structures, e.g. at the SW (0–4 km) of P036 (Fig. 3). The estimated heat flow is slightly enhanced in this area (Fig. 12). This indicates that the BSR has not yet adjusted to the new seafloor depth and is still too shallow. Hence the slumping must have occurred relatively recently, probably within the last few 1000 years. However, there is no indication of seep structures within the slump area, the BSR being clear and continuous.

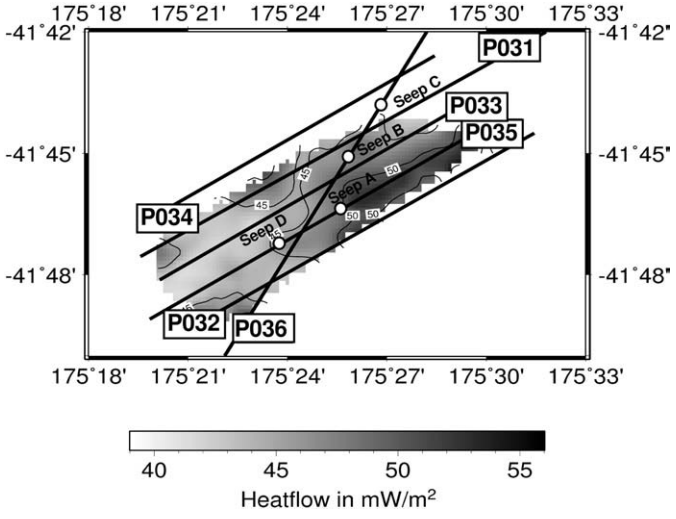

Fig. 12. Heat flow map of the study area. Black lines indicate multichannel seismic profiles. The BSR has been picked on all line, except P034 and interpolated between observed occurrences. Heat flow has then been calculated based on the BSR depth bsf with the program CSMHYD (Sloan, 1998) and using an averaged thermal conductivity of 1.2 W/m K. Note the slight increase in heat flow at the SW ends of lines P031, P032 and P036.

Another factor considered here for seep formation is the dip of stratigraphic layers. The near-horizontal migration of gas along stratigraphic layers towards the seafloor has been described e.g. for the area off Peru (Pecher et al., 2001; Netzeband et al., 2005), off Angola (Gay et al., 2007) and at the Hikurangi Margin (Lewis and Marshall, 1996; Pecher et al., 2004). This layer-parallel fluid migration is expressed in seismic anomalies by high-amplitude bright spots or a phase reversal. A phase reversal is not found in any of our profiles, but bright spots occur not only where we expect the BGHSZ, but also in shallower depths. We infer that, although there may be some migration along gently dipping stratigraphic layers, it is not a major factor in seep formation in this area.

Finally, seeps in other areas have been related to structural features such as faults, polygonal faults and anticlines (e.g. Loncke et al., 2004; Schroot et al., 2005; Léon et al., 2006; Hustoft et al., 2007). The seismic records provide only limited penetration below the BGHSZ, so that an analysis of deeper structures is difficult. A relatively prominent anticline is observed in the SW on line P035 at about 2.5 s TWT roughly between 1 km and 4 km (Fig. 2) and on P036 at 4 km, the top of the anticline at approx. 2.0 s TWT (Fig. 3). This feature is not accompanied by increased seep density and none of the seeps observed in this study is located near the top of this anticline. Structural faults are largely absent in our seismic records, which complies with the findings of Barnes et al. (this issue). They show major thrust faults north and south of Opouawe Bank, but only small faults beneath the bank itself. Hence we propose that deeper structures and faults do not play a role in the distribution of seeps on Opouawe Bank, although they might generally contribute to the methane supply. Small faults or fractures are observed in the vicinity of every identified seep structure. They sometimes reach the seafloor and sometimes stop well beneath it (Figs. 4, 6–8). It is possible that these faults continue out of plane, but this cannot be resolved. The faults

Please cite this article as: Netzeband, G.L., et al., The structures beneath submarine methane seeps: Seismic evidence from Opouawe Bank, Hikurangi Margin, New Zealand, Mar. Geol. (2009), doi:10.1016/j.margeo.2009.07.005

usually pierce the BGHSZ and hence present pathways for fluids rising from below into the BGHSZ. This mechanism has been described by Sibson (1992) as fault valve behaviour. If the hydrostatic pressure at the BGHSZ reaches the lithostatic pressure, the overpressure can be released through a fault or crack and free gas can rise into the GHSZ.

We conclude that all seep structures are correlated with small faults, which provide a path into the BGHSZ and further up to the seafloor. They present the dominant factor in the formation of seeps at this part of the Hikurangi Margin.

5.2. Tui and Tieke area

A different setting apparently exists at the area around the seeps Tui and Tieke imaged on line P036 (Figs. 3, 5c, 7). The bathymetric depression shows an acoustically high-reflective center (Fig. 5c), probably related to seep Tieke. The enhanced reflectivity is probably related to authigenic carbonate precipitation (Bialas et al., 2007). A single prominent fault impinges at the seafloor at an anticline on P036, Seep Structure C (Figs. 3 and 7). This feature is slightly different from other seeps in the research area. Firstly, this is the only seep in the study area located in a depression, even if this depression is located on the top of Opouawe Bank. Secondly, the fluid supply seems to be along a path dipping at only 6°, instead of through a vertical chimney. This oblique path probably represents a fault; reflections show an offset at the fault plane. It can be traced clearly to a depth of 1.6 s TWT, but a further continuation down to 1.9 s TWT, which corresponds to the BSR level, seems plausible. Thus, this fault probably serves two purposes. Firstly, it serves as a fluid path to the seafloor. Secondly, the formation of the depression is probably caused by movement of the blocks. The methane concentration measured at this seep site was the highest in the entire area (Krabbenhoeft et al., this issue), hence the low dip of the fault does not reduce the rate of venting.

5.3. Appearance of seep structures

We see varying appearances of seep structures in the study area: We see small mounds, seep structures terminating in a flat seafloor (Fig. 4), seismic chimneys with acoustic blanking (Figs. 4, 6), and high-amplitude reflections between the BGHSZ and the seafloor (Figs. 4, 6, 8). Léon et al. (2006) also observed different fluid escape structures in the Gulf of Cadiz. They found mud volcanoes, carbonate mounds and pockmarks. They postulated a different origin for the different structures: mounds are built up during slow rates of venting, while the pockmarks are formed during episodic events of gas hydrate dissociation. An episodic event of hydrate dissociation as assumed by Léon et al. (2006) is very unlikely since the depth of the BGHSZ is at least 300 m bsf in the study area. Hence, the different seep structures must have a different origin.

The high-amplitude reflections at the seafloor and in the upper 25 m of the sediment observed in the Parasound can be attributed to carbonate concretions. They could also be attributed to gas hydrate depositions or the interface between gas hydrate and free gas, respectively. Visual seafloor observations have shown massive sedimentation at Tui and Tieke (Bialas et al., 2007). We thus surmise that the high-amplitude patches at the seafloor are caused by authigenic carbonates. Hence, we infer that the small mounds observed at Seep Structures B and D can also be attributed to carbonate formations, so that a seep at a flat seafloor is probably young, having not yet formed a carbonate crust.

But what about the strong reflections at 10 m bsf (Seep Structure A) and 25 m bsf (Seep Structure D)? Are they caused by carbonates as well or by shallow gas hydrate, or a combination of both as suggested for pockmarks in the northern Congo Fan by Sahling et al. (2008)? Since massive carbonates have been observed at the seafloor, it seems likely that carbonate has been generated for a long time and has been buried in the course of time. Authigenic carbonates can be formed below the seafloor, but usually at depth of less than a few meters (Bayon et al., 2007; Luff et al., 2004). Therefore the high-amplitude reflections we see at Seep Structures A, C and D (Figs. 5 and 9) at depths of up to 25 m are probably buried, old carbonate crusts, from a previous time of seep activity.

In the Lower Congo Basin, Gay et al. (2007) found evidence of episodic seep activity with 29% of the seeps they found proved presently inactive. If indeed the strong reflections are from buried authigenic carbonate crusts, then they were probably buried during an inactive phase. However, continuous activity and carbonate formation, along with continuous sedimentation is also possible and would explain a horizontally very confined (max. 100 m wide) carbonate cementation reaching down 10 m bsf as seen at Seep Structure A. According to Luff et al. (2004), for the formation of carbonate crust, a relatively slow (20–90 cm/a) but pervasive (100–500 years) upward flow of methane-charged (>50 mM CH_4) fluids is necessary. High sedimentation rates (>0.5 mm/a), in contrast, inhibit crust formation. We do not have information about the exact sedimentation rate on Opouawe Bank, but on the Bank it was probably rather low. For a continuous precipitation of the carbonate crust at Seep Structure A with a maximum sedimentation rate of 0.4 mm/a, a persistent methane flux with the required velocity and concentration for at least 25,000 years would have been necessary. A possibly more realistic scenario could be a succession of carbonate precipitation phases with short breaks inbetween.

The mound at Seep Structure D (Fig. 8) represents another setting with its cementation at 25 m depth (Figs. 5a and 9) and gas accumulation below the seafloor, evidenced by the low velocity (Fig. 11). The highly reflective seafloor, noticeable in high-resolution profiles (Fig. 9), could indicate a thin carbonate crust right at the seafloor, which could serve as a seal for the gas beneath it. This process is called self-sealing (Hovland, 2002). The buried crust indicates previous activity of this seep. Either the sedimentation rate at this seep increased above that conducive to carbonate formation, or the seepage rate or methane concentration has decreased.

5.4. Coupled seeps?

The close proximity of some seeps, as observed at Seep Structure C and Seep Structure D poses the question whether these seeps represent individual seeps or coupled systems of fluid transport. Berndt (2005) describes a scenario, in which the fluids are transported through a dense net of polygonal faults which are confined to a certain layer. Above this layer, fluid migration proceeds in individual pipes. Gay et al. (2006) describe a fluid flow pattern, where the migrating gas accumulates beneath a gas hydrate seal marked by a BSR. Then the gas rises through a highly faulted interval along these faults. Both authors delineate a setting, in which gas is transported up to a certain level, where it accumulates, before it continues to the seafloor. On P035 and P036, a broad accumulation of gas beneath the BGHSZ is indicated by the noticeable signal attenuation. The individual pipes only appear above the BGHSZ. Hence a coupling of fluid paths below this level is most likely. But the ascending bright spots we see within the GHSZ at Seep Structure A and D (Figs. 4 and 8) could also mark such levels where gas is temporarily trapped. Fig. 10 shows a more detailed image of Seep Structure D, the steep reflections crossing the BGHSZ could be associated with rising fluids. It is conceivable that gas, which has crossed into the GHSZ through small faults and fractures, accumulates at the bright spots and feeds the chimneys rising above these bright spots. Thus, the seeps at Seep Structure D would be partly coupled, up to the shallowest bright spot in about 300 m bsf. A much more shallow coupling also seems feasible (Fig. 9). Gas could rise vertically through the seep structure at 7 km until about 40 m bsf and then migrate SW at a low angle of maybe 4° to the gas pocket at 6.5 km.

Please cite this article as: Netzeband, G.L., et al., The structures beneath submarine methane seeps: Seismic evidence from Opouawe Bank, Hikurangi Margin, New Zealand, Mar. Geol. (2009), doi:10.1016/j.margeo.2009.07.005

6. Conclusion

Within the New Vents project, Opouawe Bank has been proven a very active seep area. Locations of seep structures are linked to the absence of a BSR, because rising gas probably inhibits gas hydrate formation by perturbing the temperature field. Almost vertical small faults represent the main structural control on the focused fluid flow in the area of Opouawe Bank. They act as a gas conduit through the BGHSZ to the seafloor. However, the Seep Structure C (Seep Tieke) presents an exception. Its formation is probably controlled by a slant fault (6°), which is likely to act as a fluid pathway to the seafloor. The small mounds we see above some of the seep structures are attributed to authigenic carbonates. A flat seafloor at a seep site is inferred to represent a younger vent history. The buried carbonate crust of Seep Structures A, C and D accordingly relates to a previous time of seep activity, showing that the study area has a history of methane venting. Seeps can be interlinked below the seafloor or at the bright spots levels, when gas crosses into the GHSZ through small faults and fractures, accumulates at these bright spots and rises through separate chimneys above.

Acknowledgements

We would like to thank the captain, crew and scientific staff of *RV SONNE*, SO191, for the excellent support. Jan Grobys, Keith Lewis and an anonymous reviewer greatly improved the manuscript with their comments and suggestions. Thanks to Jens Greinert who added the final touch. The New Vents project was funded by the German Ministry of Education and Research (BMBF).

References

Barnes, P.M., Mercier de Lépinay, B., 1997. Rates and mechanics of rapid frontal accretion along the very obliquely convergent southern Hikurangi margin, New Zealand. J. Geophys. Res. 102, 24931–24952.

Barnes, P.M., Lamarche, G., Bialas, J., Henrys, S., Pecher, I.A., Netzeband, G.L., Greinert, J., Mountjoy, J.J., Pedley, K.,Crutchley, G.J. Tectonic and geological framework for gas hydrate and cold seeps on the Hikurangi subduction margin, New Zealand. Marine Geology, this issue.

Bayon, G., Pierre, C., Etoubleau, J., Voisset, M., Cauquil, E., Marsset, T., Sultan, N., Le Drezen, E., Fouquet, Y., 2007. Sr/Ca and Mg/Ca ratios in Niger Delta sediments: implications for authigenic carbonatenext term genesis in cold seep environments. Mar. Geol. 241, 93–109. doi:10.1016/j.margeo.2007.03.007.

Berndt, C., 2005. Focused fluid flow in passive continental margins. Phil. Trans. R. Soc. A 363, 2855–2871.

Bialas, J., Greinert, J., Linke, P., Pfannkuche, O., 2007. FS SONNE cruise report SO191 New Bents- "Puaretanga Hou", IFM-GEOMAR Report, 9, 190 pp., ISSN: 1614-6298, pp. 90, 129.

Cochonat, P., Cadet, J.-P., Lallemant, S.J., Mazzotti, S., Nouzé, H., Fouchet, C., Foucher, J.P., 2002. Slope instabilities and gravity processes in fluid migration and tectonically active environment in the eastern Nankai accretionary wedge (KAIKO-Tokai '96 cruise). Mar. Geol. 187, 193–202.

Collot, J.Y., Delteil, J., Lewis, K.B., Davy, B., Lamarche, G., Audru, J.-C., Barnes, P., Chanier, F., Chaumillon, E., Lallemand, S., Mercier de Lepinay, B., Orpin, A., Pelletier, B., Sosson, M., Toussaint, B., Uruski, C., 1996. From oblique subduction to intra-continental transpression: structures of the southern Kermadec–Hikurangi margin from multibeam bathymetry, side-scan sonar and seismic reflection. Mar. Geophys. Res. 18, 357–381. doi:10.1007/BF00286085.

Collot, J.-Y., Lewis, K., Lamarche, G., Lallemand, S., 2001. The giant Ruatoria debris avalanche on the northern Hikurangi margin, New Zealand: result of oblique seamount subduction. J. Geophys. Res. 106, 19271–19297.

Dupré, S., Woodside, J., Foucher, J.-P., de Lange, G., Mascle, J., Boetius, A., Mastalerz, V., Stadnitskaia, A., Ondréas, H., Huguen, C., Harmégnies, F., Gontharet, S., Loncke, L., Deville, E., Niemann, H., Omoregie, E., Olu-Le Roy, K., Fiala-Medioni, A., Dählmann, A., Caprais, J.-C., Prinzhofer, A., Sibuet, M., Pierre, C., Damsté, J.S., the NAUTIL Scientific Party, 2007. Seafloor geological studies above active gas chimneys off Egypt (Central Nile Deep Sea Fan). Deep Sea Res. I 54, 1146–1172. doi:10.1016/j.dsr.2007.03.007.

Eichhubl, P., Green, H.G., Naehr, T., Maher, N., 2000. Structural control of fluid flow: offshore fluid seepage in the Santa Barbara Basin, California. J. Geochem. Explor. 69/70, 545–549.

Etiope, G., Klusman, R.W., 2002. Geologic emissions of methane to the atmosphere. Chemosphere 49, 777–789.

Etiope, G., Milkov, A.V., Derbyshire, E., 2007. Did geologic emissions of methane play any role in Quaternary climate change? Global. Planet. Change 61, 79–88.

Faure, K., Greinert, J., Pecher, I.A., Graham, I.J., Massoth, G.J., deRonde, C.E., Wright, I.C., Baker, E.T., Olson, E.J., 2006. Methane seepage and its relation to slumping and gas hydrate at the Hikurangi margin, New Zealand. N.Z. J. Geol. Geophys. 49, 503–516.

Faure, K., Greinert, J., Schneider v.D., J., McGinnis, D.F., Kipfer, R., Linke, P., this issue. Free and dissolved methane in the water column and the sea surface: Geochemical and hydroacoustic evidence of bubble transport. Mar. Geol.

Field, B.D., Uruski, C.I., Beu, A., Browne, G., Crampton, J., Funnel, R., Killops, S., Laird, M., Mazengarb, C., Morgans, H., et al., 1997. Cretaceous–Cenozoic geology and petroleum systems of the east coast region, New Zealand. Lower Hutt, New Zealand, Institute of Geological and Nuclear Sciences. 301 pp.

Gay, A., Lopez, M., Cochonat, P., Séranne, M., Levaché, D., Sermondadaz, G., 2006. Isolated pseafloor pockmarks linked to BSRs, fluid chimneys, polygonal faults and stacked Oligocene–Miocene turbiditic paleochannels in the Lower Congo Basin. Mar. Geol. 226, 25–40.

Gay, A., Lopez, M., Berndt, C., Séranne, M., 2007. Geological controls on focused fluid flow associated with seafloor seeps in the Lower Congo Basin. Mar. Geol. 244, 68–92.

Giggenbach, W.F., Stewart, M.K., Sano, Y., Goguel, R.L., Lyon, G.L., 1993. Isotopic and chemical composition of the waters and gases from the East Coast accretionary prism, New Zealand. Proceedings of the Final Research Coordination Meeting on the Application of Isotope and Geochemical Techniques to Geothermal Exploration in the Middle East, Asia, the Pacific and Africa, pp. 208–231.

Greinert, J., Artemov, Y., Egorov, V., De Batist, M., McGinnis, D., 2006a. 1300-m-high rising bubbles from mud volcanoes at 2080 m in the Black Sea.: hydroacoustic characteristics and temporal variability. Earth and Planet. Sci. Lett. 244, 1–15.

Greinert, J., Lewis, K., Bialas, J., Pecher, I., Rowden, A., Linke, P., De Batist, M., Bowden, D.A., Suess, E. Methane seepage along theHikurangi Margin, New Zealand: review of studies in 2006 and 2007. Mar. Geol., this issue.

Henrys, S., Ellis, S., Uruski, C., 2003. Conductive heat flow variations from bottom simulating reflectors on the Hikurangi margin, New Zealand. Geophys. Res. Lett. 30, 1065–1068. doi:10.1029/2002GL015772.

Hovland, M., Gardner, J.V., Judd, A.G., 2002. The significance of pockmarks to understanding fluid flow processes and geohazards. Geofluids 2, 127–136.

Hovland, M., 2002. On the self-sealing nature of marine seeps. Cont. Shelf Res. 22, 2387–2394.

Hustoft, S., Mienert, J., Bünz, S., Nouzé, H., 2007. High-resolution 3D-seismic data indicate focussed fluid migration pathways above polygonal fault systems of the mid-Norwegian margin. Mar. Geol. 245, 89–106.

Judd, A.G., Hovland, M., Dimitrov, L.I., Garcia Cil, S., Jukes, V., 2002. The geological methane budget at Continental Margins and its influence on climate change. Geofluids 2, 109–126.

Judd, A.G., 2003. The global importance and context of methane escape from the seabed. Geo-Mar. Lett. 23, 147–154. doi:10.1007/s00367-003-0136-z.

Katz, H.R., 1981. Probable gas hydrate in continental slope east of the North Island, New Zealand. J. Pet. Geol. 3, 315–324.

Katz, H.R., 1982. Evidence for gas hydrates beneath the continental slope, East Coast, North Island, New Zealand. N.Z. J. Geol. Geophys. 25, 193–199.

Klaucke, I., Weinrebe, W., Petersen, C.J., Bowen, D. Temporal variability of gas seeps offshore New Zealand: multi-frequency geoacoustic imaging of the Wairarapa area, Hikurangi margin. Marine Geology, this issue.

Krabbenhoeft, A., Netzeband, G.L., Bialas, J., Papenberg, C. Methane concentrations from ocean bottom stations and their relation to seismic structures. Marine Geology, this issue.

Kvenvolden, K.A., Pettinga, J.R., 1989. Hydrocarbon gas seeps of the convergent Hikurangi margin, North Island New Zealand. Mar. Pet. Geol. 6, 2–8.

Léon, R., Somoza, L., Medialdea, T., Maestro, A., Díaz-del-Río, V., del Carmen Fernández-Puga, M., 2006. Classification of sea-floor features associated with methane seeps along the Gulf of Cádiz continental margin. Deep-Sea Res. II 53, 1464–1481.

Lewis, K.B., Marshall, B.A., 1996. Seep faunas and other indicators of methane-rich dewatering on New zealand convergent margins. N.Z. J. Geol. Geophys. 39, 181–200.

Lewis, K.B., Collot, J.-Y., Lallem, S.E., 1998. The dammed Hikurangi Trough: a channel-fed trench blocked by subducting seamounts and their wake avalanches (New Zealand–France GeodyNZ Project). Basin Res. 10, 441–468. doi:10.1046/j.1365-2117.1998.00080.x.

Loncke, L., Mascle, J., Fanil Scientific Parties, 2004. Mud volcanoes, gas chimneys, pockmarks and mounds in the Nile deep-sea fan (Eastern Mediterranean): geophysical evidences. Mar. Pet. Geol. 21, 669–689.

Luff, R., Wallmann, K., Aloisi, G., 2004. Numerical modeling of carbonate crust formation at cold vent sites: significance for fluid and methane budgets and chemosynthetic biological communities. Earth Planet. Sci. Lett. 221, 337–353. doi:10.1016/S0012-821X(04)00107-4.

Mazurenko, L.L., Soloviev, V.A., 2003. Worldwide distribution of deep-water fluid venting and potential occurrences of gas hydrate accumulations. Geo-Mar. Lett. 23, 12–176. doi:10.1007/s00367-003-0146-x.

Netzeband, G.L., Hübscher, C.P., Gajewski, D., Grobys, J.W.G., Bialas, J., 2005. Seismic velocities from the Yaquina forearc basin off Peru: evidence for free gas within the gas hydrate stability zone. Int. J. Earth Sci. 94, 420–432. doi:10.1007/s00531-005-0483-2.

Pecher, I.A., Kukowski, N., Huebscher, C., Greinert, J., Bialas, J., GEOPECO Working Group, 2001. The link between bottom-simulating reflections and methane flux into the gas hydrate stability zone—new evidence from Lima Basin, Peru Margin. Earth Planet. Sci. Lett. 185 (3–4), 343–354. doi:10.1016/S0012-821X(00)00376-9.

Pecher, I.A., Henrys, S.A., Zhu, H., 2004. Seismic images of gas conduits beneath vents and gas hydrates on Ritchie Ridge, Hikurangi margin, New Zealand. N.Z. J. Geol. Geophys. 47, 275–279.

Please cite this article as: Netzeband, G.L., et al., The structures beneath submarine methane seeps: Seismic evidence from Opouawe Bank, Hikurangi Margin, New Zealand, Mar. Geol. (2009), doi:10.1016/j.margeo.2009.07.005

Pecher, I.A., Ellis, S., Henrys, S.A., Chiswell, S.M., Kukowski, N., 2005. Erosion of the seafloor at the top of the gas hydrate stability zone on the Hikurangi margin, New Zealand. Geophys. Res. Lett. 32, L24603. doi:10.1029/2005GL024687.

Reading, A.M., Gubbins, D., Mao, W., 2001. A multiphase seismic investigation of the shallow subduction zone, southern North Island, New Zealand. Geophys. J. Int. 147, 215–226.

Robinson, R., 1986. Seismicity, structure and tectonics of the Wellington region. Geophys. J. R. Astron. Soc. 87, 379–409.

Rollet, N., Logan, G.A., Kennard, J.M., O' Brien, P.E., Jones, A.T., Sexton, M., 2006. Characterisation and correlation of active hydrocarbon seepage using geophysical data sets: an example from the tropical, carbonate Yampi Shelf, Northwest Australia. Mar. Pet. Geol. 23, 145–164.

Sahling, H., Bohrmann, G., Spiess, V., Bialas, J., Breitzke, M., Ivanov, M., Kasten, S., Krastel, S., Schneider, R., 2008. Pockmarks in the Northern Congo Fan area, SW Africa: complex seafloor features shaped by fluid flow. Mar. Geol. 249, 206–225.

Schroot, B.M., Klaver, G.T., Schüttenhelm, R.T.E., 2005. Surface and subsurface expressions of gas seepage to the seabed—examples from the southern North Sea. Mar. Pet. Geol. 22, 499–515.

Schwalenberg, K.,Haeckel, M., Poort, J., Jegen, M., this issue. Evaluation of gas hydrate deposits in an active seep area using marine controlled source electromagnetics: Results from the Wairarapa area, New Zealand. Marine Geology, this issue.

Sibson, R.H., 1992. Implications of fault-valve behaviour for rupture nucleation and recurrence. Tectonophysics 211, 283–293.

Sloan, E.D., 1998. Cathrate hydrates of natural gases. Dekker, New York.

Sommer, S., Linke, P., Pfannkuche, O., Treude, T., Niemann, H., this issue. Benthic respiration in a seep habitat dominated by dense beds of ampheretid polychaetes a the Hikurangi Margin (New Zealand). Mar. Geol.

Townend, J., 1997. Estimates of conductive heatflow through bottom-simulating reflectors on the Hikurangi and southwest Fjordland continental margins, New Zealand. Mar. Geol. 141, 209–220.

Walcott, R., 1987. geodetic strain and the deformational history of the North Island of New Zealand during the late Cainozoic. Phil. Trans. R. Soc. Lond. 321, 231–277.

Zelt, C.A., Smith, R.B., 1992. Seismic traveltime inversion for 2-D crustal velocity structure. Geophys. J. Int. 108, 16–34.

Zillmer, M., Flueh, E.R., Petersen, J., 2005. Seismic investigation of a bottom simulating reflector and quantification of gas hydrate in the Black Sea. Geophys. J. Int. 161, 662–678. doi:10.1111/j.1365-246X.2005.02635.x.

Please cite this article as: Netzeband, G.L., et al., The structures beneath submarine methane seeps: Seismic evidence from Opouawe Bank, Hikurangi Margin, New Zealand, Mar. Geol. (2009), doi:10.1016/j.margeo.2009.07.005